

# DiffDoctor: Diagnosing Image Diffusion Models Before Treating

Yiyang Wang<sup>1</sup> Xi Chen<sup>1</sup> Xiaogang Xu<sup>4</sup> Sihui Ji<sup>1</sup>  
 Yu Liu<sup>2</sup> Yujun Shen<sup>3</sup> Hengshuang Zhao<sup>1,†</sup>

<sup>1</sup>The University of Hong Kong <sup>2</sup>Tongyi Lab <sup>3</sup>Ant Financial Services Group <sup>4</sup>Zhejiang University

## Abstract

In spite of the recent progress, image diffusion models still produce artifacts. A common solution is to refine an established model with a quality assessment system, which generally rates an image in its entirety. In this work, we believe **problem-solving starts with identification**, yielding the request that the model should be aware of not just the presence of defects in an image, but their specific locations. Motivated by this, we propose *DiffDoctor*, a two-stage pipeline to assist image diffusion models in generating fewer artifacts. Concretely, the first stage targets developing a robust artifact detector, for which we collect a dataset of over 1M flawed synthesized images and set up an efficient human-in-the-loop annotation process, incorporating a carefully designed class-balance strategy. The learned artifact detector is then involved in the second stage to tune the diffusion model through assigning a per-pixel confidence map for each synthesis. Extensive experiments on text-to-image diffusion models demonstrate the effectiveness of our artifact detector as well as the soundness of our diagnose-then-treat design.

## 1. Introduction

The advancement of image diffusion models [9, 13, 16, 20] has made it possible to synthesize various images based on different conditions. However, these models may still synthesize distorted, unreasonable, and unwanted content in the images, known as artifacts [5, 14, 36], as shown in Fig. 1. Unwanted artifacts make the outputs of the image diffusion models unstable, posing a significant challenge to the wider use of generative models in real-world applications.

Why do artifacts appear in synthesized images? We assert that artifacts stem from the training data’s inherent noise and the model’s limited capacity. Regarding data, diffusion models are predominantly trained on web-mined images, which are frequently noisy [3, 11]. However, standard diffusion losses [9, 16] do not differentiate between valuable supervisory signals and noise in the training data,

† Corresponding author.

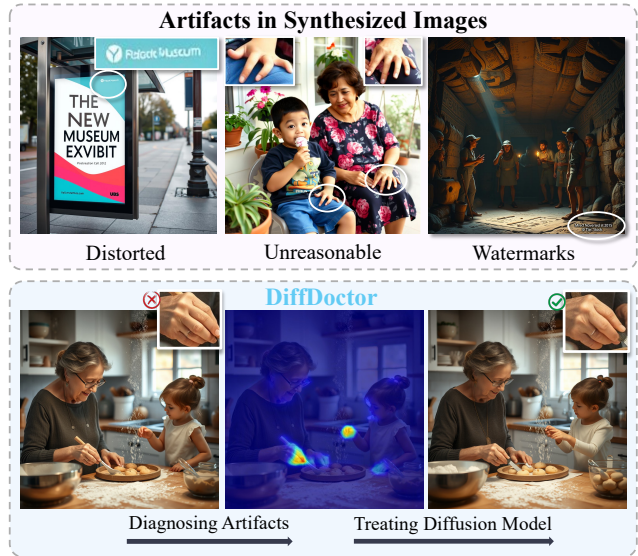


Figure 1. **Illustrations of DiffDoctor.** Image diffusion models inevitably generate artifacts. We train a robust artifact detector to diagnose the artifacts and treat the diffusion model. After treating on limited prompts, the diffusion model generates fewer artifacts of similar types on unseen prompts while maintaining the quality.

leading the model to not only learn to generate vivid images but also inadvertently learn from the noise, which manifests as artifacts during image generation. Regarding model capacity, the model’s limited capacity prevents it from fully capturing and representing complex visual details in every synthesis, occasionally resulting in artifacts. Therefore, image diffusion models have the potential to generate correct images but lack the stability to do so reliably with each synthesis. One way to refine the pre-trained model toward more stable desired outputs is by using feedback, which can be a score describing the quality of the image, and current methods attempt to maximize such score. However, feedback of these methods is generally an image-level score [4–6, 8, 12, 18, 26, 28, 37] to each image, or pairwise comparisons [24], overlooking fine-grained pixel-level information — artifacts are sparse within the image. This analysis shapes the motivation for our paper: *Problem-solving starts with identification. We should know where artifacts are before tuning the diffusion model.*

Therefore, we present `DiffDoctor`, which tunes diffusion models in a diagnose-then-treat diagram. Diagnosing means identifying the artifact locations in synthesized images, which requires an artifact detector to predict artifact confidence. Treating means supervising the diffusion model with the artifact detector, where we minimize the per-pixel artifact confidence of synthesized images, aiming to reduce artifacts in future synthesis. Illustrations are in Fig. 1.

To train a robust artifact detector, it is essential to collect comprehensive data. RichHF [14] and PAL4VST [36] provide dense artifact annotations. However, we identify severe data-imbalance issues – overwhelming positive samples on specific categories (e.g., hands are usually wrong). Training on them leads to a high false positive rate of the artifact detector in these categories (e.g., predict artifacts for every hand even when correct). Therefore, we develop a class-balancing strategy to collect additional data to balance negative and positive artifact samples. Using this strategy, we established a human-in-the-loop pipeline to collect and label images synthesized by various diffusion models. Hard cases are meticulously labeled by human annotators to ensure accurate target signals, while easier cases are auto-labeled [32] by the trained artifact detector using a specially designed augmentation strategy. Together, these efforts result in a robust artifact detector trained on 1M+ samples.

After developing a robust artifact detector, we treat the diffusion model with supervision from the artifact detector. The diagnosed artifacts are artifact confidence maps, where each pixel’s value represents the confidence (or probability) of artifact presence, which we aim to minimize. Therefore, we prompt a trainable diffusion model to synthesize images, detect artifact maps using the artifact detector, and directly back-propagate the gradients by minimizing the artifact confidence of each pixel of the synthesized images back to the diffusion model. This method leverages the pixel-level information in artifact-prone areas, allowing precise treating (or penalizing) of the diffusion model to make the model try to avoid these artifacts in the future. This diagnose-then-treat diagram could also seamlessly accommodate original diffusion losses as an auxiliary loss to regularize the model.

To the best of our knowledge, `DiffDoctor` is the first approach to use pixel-level feedback for tuning image diffusion models. Tuned on limited prompts, the diffusion model generates fewer artifacts of similar types on unseen prompts while maintaining the quality. It’s also applicable to other methods such as DreamBooth [21]. Our contributions are summarized as follows:

- We propose `DiffDoctor`, the first approach to use pixel-level feedback to tune image diffusion models to reduce artifacts using a diagnose-then-treat design.
- To diagnose artifacts, we train a robust artifact detector by using a careful class-balance strategy and scaling up the data with human-in-the-loop.

- To treat artifacts, we supervise the diffusion model with the artifact detector to minimize the per-pixel confidence of synthesized images.

## 2. Related Work

**Detect abnormality in images.** Our work focuses on detecting and thereby mitigating artifacts in *synthesized* images of diffusion models, which may be confused with detecting GenAI-generated or altered images [25, 29, 34, 35]. These works aim to identify whether AI has generated or manipulated a real image, rather than assessing the presence of artifacts within synthesized images. Now for the artifacts in synthesized images. SynArtifact [5] uses VLMs to classify artifacts or to locate them using bounding boxes. PAL4VST [36] and RichHF [14] concurrently provide the first open-sourced data with annotated artifact areas for synthesized images. However, these artifact annotations suffer from limitations of imbalance and coarse granularity, which can significantly compromise the effectiveness of an artifact detector trained on them. In this work, we carefully design a class-balance strategy and set up a human-in-the-loop annotation process, resulting in a robust artifact detector trained on 1M+ data samples.

**Guide diffusion models with feedback.** Recently, inspired by RLHF for LLMs [17], ImageReward [28] introduces an image reward model to approximate human feedback with image-level scores and optimizes diffusion models via ReFL to maximize these scores. DDPO and DPOK [4, 8] apply reinforcement learning (RL) [23] to make diffusion models maximize a global score (e.g., aesthetic score). Zhang et al. [37] is the first to apply RL at scale, training diffusion models with millions of prompts and multiple reward objectives. SynArtifact [5] globally classifies artifacts as scores and applies RL to tune diffusion models. Diffusion-DPO [24] applies direct preference optimization [19] to diffusion models, transforming the RL problem into a classification objective between winning and losing samples. AlignProp [18] and DRaFT [6] directly optimize diffusion models by back-propagating from differentiable reward models to maximize the image-level score. However, these models rely on image-level ratings or comparisons, tuning the model to maximize overall scores and overlooking the fine-grained information in each pixel. PAL4VST [36] and RichHF [14] are the first to leverage fine-grained artifact annotations. However, they don’t use these fine-grained annotations to fine-tune diffusion models; instead, they simply generate a batch of images to rank based on artifact confidence or mask out problematic areas for inpainting. In this paper, we instead diagnose pixel-level artifacts to tune (treat) diffusion models, enabling them to try to avoid generating artifacts in the future. To the best of our knowledge, `DiffDoctor` is the first approach to utilizing pixel-level feedback for tuning diffusion models.

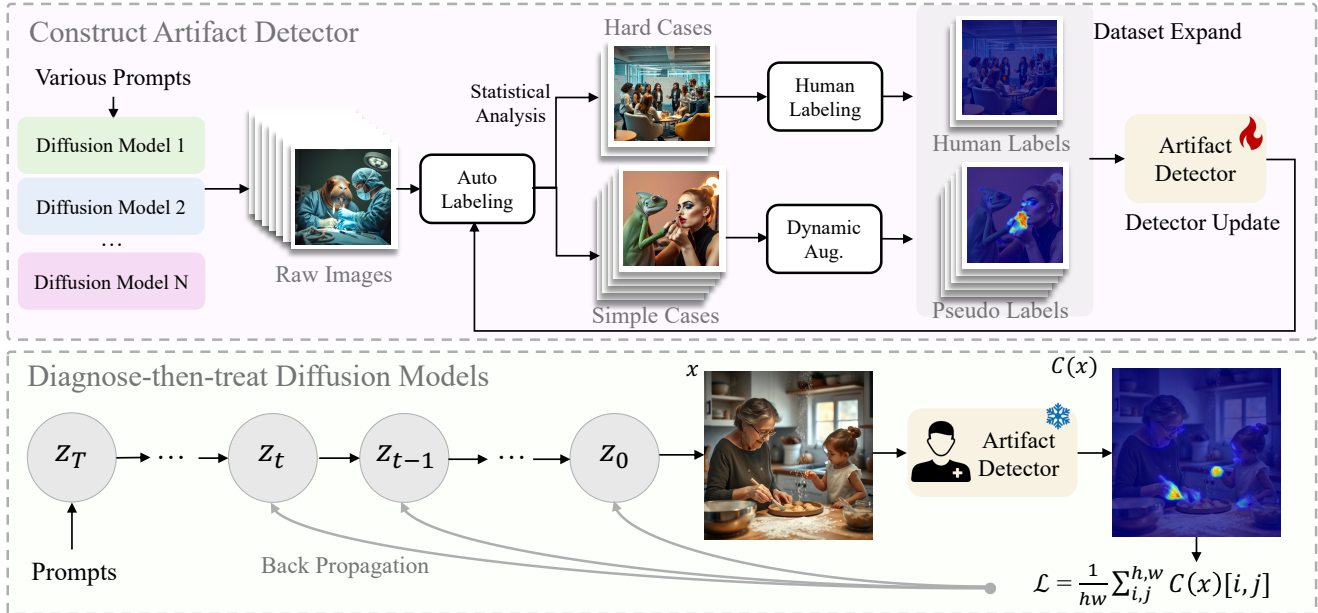


Figure 2. **Pipeline of DiffDoctor.** The first part shows the training of an artifact detector – the doctor. Starting with the initial dataset, the artifact detector is trained in a humans-in-a-loop manner. The second part shows our diagnose-then-treat design, where the patient – a trainable diffusion model, is prompted to synthesize images. Then the frozen artifact detector diagnoses its result by predicting the artifact maps, on which it treats the patient by minimizing the per-pixel artifact confidence to back-propagate to the diffusion model.

### 3. Method

#### 3.1. Preliminaries

**Artifact definition.** We define artifacts as three types: shape distortions (*e.g.*, distorted hands, faces, words), unreasonable content (*e.g.*, extra limbs, more-or-fewer fingers), and watermarks. We don’t consider artifacts requiring complex reasoning to find (*e.g.* floating objects without physical support). Examples of artifacts are in Fig. 1.

**Artifact detection.** We define artifact areas in synthesized images as confidence maps (artifact maps), transforming artifact detection problems into a binary segmentation task, where each pixel represents a confidence value from 0 to 1, indicating the likelihood of the pixel being part of an artifact. Then the training process of the artifact detector is to minimize the mean squared error (MSE) loss between the predicted artifact maps and the ground truth artifact maps:

$$\mathcal{L}_{AD}(\theta) = \frac{1}{N} \sum_{i=1}^N \left\| \hat{C}_{\theta}(x_i) - C(x_i) \right\|_2^2, \quad (1)$$

where  $N$  is the number of samples in a batch,  $x_i$  is the  $i$ -th synthesized image,  $C(x_i)$  is the ground truth artifact map of  $x_i$ , and  $\hat{C}_{\theta}(x_i)$  is the predicted artifact map of  $x_i$ .

#### 3.2. Construct Artifact Detector

We find an imbalance of current artifact annotations compromising the artifact detector, so we design a class balance strategy with human-in-the-loop to train a robust artifact

detector on 1M+ balanced data samples. The pipeline for constructing artifact detector is in Fig. 2: We generate numerous images using various diffusion models, selecting hard cases for human labeling through statistical analysis, while simpler cases are automatically labeled by the updated artifact detector following semi-supervised learning.

**Data-imbalance issue.** Existing datasets with pixel-level artifact annotations [14, 36] provide synthesized images with artifact maps, offering a training set of 25K samples and establishing a foundation for artifact detector construction. However, we identify a limitation due to data imbalance in previous data, which seriously compromises the performance of the artifact detector. Specifically, the negative (artifact-free) and positive (artifact-prone) samples are significantly unbalanced in certain categories. For instance, human-centered images synthesized with inferior models or without careful prompting are likely to exhibit distorted hands or faces (artifacts), which dominate the training set in previous datasets. Such overwhelming positive samples cause the artifact detector to learn a shortcut, leading it to predict high artifact confidence in the face and hand regions, even for normal hands and faces, resulting in high false positive rates for these hard categories. This issue is unnoticed because the testing set is also imbalanced, which obscures the high false positive rates during evaluation.

**Balance data distribution.** We first incorporate high-quality real photos as negative samples to balance the distribution, as they are artifact-free, easy to obtain, and don’t require labeling. After adding real images, the false positive rate of the artifact detector on real photos reduces

significantly. However, this data still has limitations in generalizing to synthesized images due to the domain gap. Therefore, we further incorporate synthesized images.

Different from label-free real photos, synthesized images require dense annotations for artifact areas. Given the expensive cost of extensively labeling artifact areas, we only label the most informative and hard cases that are challenging for artifact detectors to learn. The imbalance problem arises because prompts for certain categories (*e.g.*, humans, texts) are hard for diffusion models to generate, resulting in synthesized images naturally lacking negative samples, so are also hard for artifact detectors to discriminate. We find these hard categories by classifying using VQA models [2] and find the categories with abnormally higher predicted artifact confidence. Then we use an LLM [1] to generate various prompts for these categories and synthesize images using SOTA text-to-image models. Images synthesized by these models contain numerous challenging positive cases and negative cases for the artifact detector. From them, we select a subset of 2k hard cases by thresholding the images detected with high artifact confidence on these categories, which we then manually label to provide precise guidance signals for joint training.

**Scale-up with unlabeled images.** To further enhance the generalization ability and robustness of the artifact detector, we scale up the training data by predicting pseudo-labels for the images not selected as hard cases, following studies in semi-supervised learning [30–33]. Illustrated in the first part of Fig. 2, we jointly train the artifact detector on both true labels and pseudo labels with humans in the loop, resulting in 1M+ data samples involved in training. We also design a dynamic augmentation strategy specifically for artifact detection to perturb the pseudo labels.

The dynamic augmentation strategy involves shrinking only images with a predicted maximum artifact confidence value below a certain threshold to smaller sizes, and then padding them back to original sizes. This is because an inferior artifact detector tends to falsely predict high artifact confidence on small intricate regions (*e.g.*, faces and hands in full body images). Whereas, large areas predicted with low artifact confidence (*e.g.*, close-up portraits) are more likely to be correct. Therefore, these shrunk images are transformed into small intricate areas with a high likelihood of low artifact confidence, which helps to balance the distribution. Apart from this dynamic strategy, we apply strong augmentations for pseudo labels following semi-supervised learning studies [31, 32].

**Robust artifact detector.** The above content demonstrates how we balance and scale up the data. In terms of model backbone selection, we train our artifact detector using SegFormer-b5 [27] as the backbone. We directly apply a sigmoid function after the logit outputs to get confidence values for each pixel, which is output as the artifact map.

### 3.3. Diagnose-then-treat Diffusion Models

The artifact detector enables us to diagnose artifacts within synthesized images, serving as valuable dense supervisory signals for artifacts. Although RichHF [14] and PAL4VST [36] also attempt to locate artifacts in synthesized images, they just use this information to inpaint problematic areas or to rank batches of images. How to leverage these pixel-level artifacts to supervise diffusion models remains underexplored. Therefore, we present pixel-aware treating, which tunes the diffusion model with the supervision from the artifact detector as shown in Fig. 2. **Pixel-aware treating.** The artifact detector is differentiable, so we can directly back-propagate gradients from detected artifact maps of synthesized images to the diffusion model through the artifact detector. We aim to minimize all confidence of the artifact map of the synthesized image (*i.e.*, punish high artifact confidence), leading to the following pixel-aware loss for supervising the diffusion model:

$$\mathcal{L}_{\text{pixel}}(\theta) = \frac{1}{h \times w} \sum_{i,j} C(\pi_{\theta}(z_T))[i, j], \quad (2)$$

where  $\pi_{\theta}(z_T)$  represents the image sampled from the *whole* denoising process of a pre-trained diffusion model starting from a standard Gaussian noise  $z_T$ . Note that the diffusion model performs the denoising process with gradient tracking.  $C(\pi_{\theta}(z_T))$  is the artifact map of this synthesized image diagnosed by the artifact detector,  $h, w$  are the height and width, and  $i, j$  traverse all pixel coordinates. This loss supervises the diffusion model on all pixel-level artifacts from the artifact detector to suppress the diffusion model for generating high artifact confidence areas. *i.e.*, treat it to exclude artifacts. Illustration is shown in Fig. 2

Following studies of direct reward fine-tuning [6, 18] which also directly back-propagating diffusion models but with global reward models when doing full-chain sampling, we truncate the gradients in the last few steps in the denoising chain to save memory.

**Compatibility with diffusion loss.** Pixel-aware treating is also seamlessly compatible with standard diffusion losses, which can also help delay the model collapse. Regarding collapse, overly treating the model will lead to quality degradation (model collapse) similar to the reward hacking problem, as discussed in Sec. 4.2. We can avoid this problem by using early stopping; however, we still consider minimizing KL regularization to constrain updated models from the real image distribution to mitigate collapse:  $\mathbb{E}_{p(y)}[\text{KL}(p_{\theta}(x|y)||p_{\text{real}}(x|y))]$ , which can be transformed into a rectified flow loss [7, 16]:

$$\mathcal{L}_{\text{offline}}(\theta) = \|(z_T - z_0) - v_{\theta}(z_t, t)\|. \quad (3)$$

We call it an offline regularization term and derive the final

---

**Algorithm 1** DiffDoctor w/ Offline Regularization

---

```
1: Prompt Set:  $\mathcal{C} = \{c_1, c_2, \dots, c_n\}$ 
2: Real Image Set:  $\mathcal{D} = \{I_1, I_2, \dots, I_m\}$ 
3: Input: Base diffusion model with pre-trained parameters  $\theta_0$ ,
   artifact detector  $\mathcal{AD}$ , regularization scale  $\gamma$ 
4: Initialization: Noise scheduler timestep number  $T$ , gradient
   truncation time step  $t_{tr}$ 
5: while not converged do
6:   for  $c_j \in \mathcal{C}$  do
7:      $z_T \sim \mathcal{N}(0, \mathbf{I})$ 
8:     for  $i = T, \dots, t_{tr} + 1$  do
9:       no grad:  $z_{i-1} \leftarrow p_\theta(z_i|i; c_j)$ 
10:    end for
11:   for  $i = t_{tr}, \dots, 1$  do
12:     with grad:  $z_{i-1} \leftarrow p_\theta(z_i|i; c_j)$ 
13:   end for
14:    $x \leftarrow \text{VAEdec}(z_0)$  ▷ Decode the image
15:    $C(x) \leftarrow \mathcal{AD}(x)$  ▷ Get the artifact map
16:    $\mathcal{L}_{\text{pixel}} \leftarrow \overset{\text{aggregate}}{C}(x)$  ▷ Pixel-aware loss
17:    $I_k \leftarrow \text{select}(\mathcal{D})$  ▷ Select a real image
18:    $\mathcal{L}_{\text{offline}} \leftarrow \overset{\text{diffusion}}{I_k}$  ▷ standard diffusion loss
19:    $\mathcal{L} \leftarrow \mathcal{L}_{\text{pixel}} + \gamma \mathcal{L}_{\text{offline}}$  ▷ Final loss
20:    $p_{\theta_{i+1}} \leftarrow p_{\theta_i}$  ▷ Update the diffusion model
21: end for
22: end while
```

---

loss with the regularization:

$$\mathcal{L} = \mathcal{L}_{\text{pixel}} + \gamma \mathcal{L}_{\text{offline}}, \quad (4)$$

where we empirically choose  $\gamma = 0.25$ . In this case,  $\mathcal{L}_{\text{pixel}}$  is seamlessly fused with a diffusion loss, and only one diffusion model is required to load, which just slightly increases the training overhead for treating. We further discuss its effect in Sec. 4.2. The pseudocode of DiffDoctor with the offline regularization term is shown in Algorithm 1, where “no grad” stands for disabling gradient tracking and “with grad” performs gradient tracking.

## 4. Experiments

### 4.1. Experiment Settings

**Artifact detector benchmark.** RichHF has a testing set of 955 images, but their labels are circles with fixed radii. These fixed-radius circles sometimes cover non-artifact areas redundantly and sometimes fail to fully cover the entire artifact, leading to inaccurate metric values. Therefore, we do not use this benchmark and we construct a benchmark of 771 images. It contains synthesized images covering hard cases challenging for artifact detectors with fine-grained artifact labels, and real photos from COCO [15] testing set to measure the false positive rates on real photos. For the metrics, we use MSE to measure accuracy. To measure the false negative rates, we utilize the mean KL divergence:



original image ground truth only previous + hard cases + pseudo 1M

Figure 3. **Qualitative ablation study of artifact detectors.** We visualize the artifact maps predicted by the artifact detector on our hard benchmark by headmaps.

$\text{KL}(P||Q) = \frac{1}{N} \sum_{\text{pixels}} [p(x) \log \frac{p(x)}{q(x)}]$  where  $p(x)$  and  $q(x)$  are the ground truth and predicted confidence for pixel  $x$ ,  $N$  is total pixel number. Relatively,  $\text{KL}(1 - P||1 - Q) = \frac{1}{N} \sum_{\text{pixels}} [(1 - p(x)) \log \frac{(1 - p(x))}{(1 - q(x))}]$  is effective in measuring false positive rates, and we denote this metric as KL(1-) in the following sections.

**Model treating dataset.** The training set and the benchmark for treating only contain text prompts. We prompt Qwen [1] to synthesize 3100 complex prompts describing complicated and various scenarios mainly concerning human activities, animals, and words in life to challenge the diffusion models. We randomly break them into a training set of 3000 prompts, and a benchmark of 100 prompts. For offline regularization, we use LAION-Aesthetics V2 6.5+ Dataset [22] to regularize the model on high-quality aesthetic images. For the metrics, we detect and calculate the average of all mean or max artifact confidence across all artifact maps of synthesized images in evaluation. For image quality, we adopt the ImageReward score [28]. We also conducted user studies with 24 users. We offer them pairs of images on the same backbone model before and after treating and ask them to select a winning image based on general image quality and artifact presence respectively. Then we calculate the winning rate before and after treating. **Implementation details.** For the diffusion model to treat, we mainly use FLUX.1 Schnell [13] and use an inference step of 5. We use a learning rate of  $1e - 4$ . To save memory, we choose the gradient truncation timestep  $t_{tr}$  to be 1 and only train LoRA [10] layers (LoRA rank is 16). We use the best artifact detector (+ pseudo 1M) for training. We also try Stable Diffusion 1.5 (SD1.5) [20] which produces images of lower quality for more observations.

### 4.2. Ablation Studies

**Artifact detector.** When solely trained on the training set of previous artifact annotations, the model demonstrates high false positive rates (KL(1-)) and high MSE in our bench-

Method	MSE Ours↓	KL Ours↓	KL(1-) Ours↓	MSE real↓	KL(1-) real↓
only previous	1.601	1.059	7.044	0.979	6.082
+ real photos	1.167	1.111	4.803	0.029	1.558
+ hard cases	0.504	<b>0.981</b>	2.983	0.003	0.458
+ pseudo 4K	0.414	1.031	3.250	0.003	0.401
+ pseudo 1M	<b>0.337</b>	1.004	<b>2.231</b>	<b>0.002</b>	<b>0.371</b>

Table 1. **Quantitative ablation study of artifact detectors.** Data are displayed in percentages with percentage signs (%) omitted. We measure on **our** constructed benchmark and **real** photos.

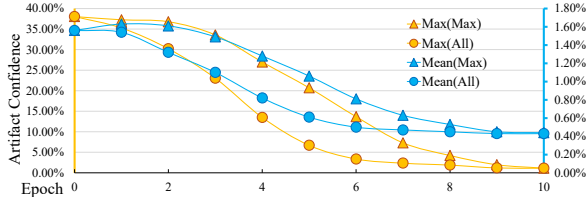


Figure 4. **Gradient selection for treating.** “Mean(Max)” means, predicting artifact maps of images generated by the model treated with the **max** confidence pixel, and then calculating the average of the **mean** confidence across all artifact maps. Epoch 0 means results of the model (FLUX.1) before DiffDoctor.

mark and real photos in Tab. 1, which is also visualized in Fig. 3 as the model outputs high confidence for almost all the face and limb areas. Balanced with real photos, the false positive rate is reduced on real photos but still is high for our synthesized image benchmark. Incorporating hard cases into training further improves the model’s MSE and reduces false positive rates. A great enhancement is shown in Fig. 3, where adding hard cases significantly mitigates the shortcut problem, preventing the model from over-detecting face and limb areas and directing its focus more accurately on true artifacts. The careful human labeling data also enables the model to produce artifact predictions of finer granularity that are not circular areas with fixed radii.

We further experiment with different numbers of pseudo labels for training (4K and 1M). Incorporating pseudo-labeled images further reduces false positive rates and MSE on both our benchmark and real photos, with performance improving as more pseudo-labels are included. We also observe that using pseudo-labels will slightly increase the KL values (false negative rates). We hypothesize that this is due to the increasing negative signals in pseudo labels, causing the model to become slightly more conservative in predicting high confidence. However, given the significant improvements in accuracy and false positive rates that cover the slight degradation of false negative rates, we choose the model trained on 1M+ pseudo labels as the best artifact detector used for the following experiments for treating.

**Pixel-aware treating.** DiffDoctor enables a finer gradient selection for pixels by assigning weights (or masks) on the artifact confidence for each pixel in  $\mathcal{L}_{\text{pixel}}$  during pixel-aware treating. Using FLUX.1, we compare the approach of selecting the gradients of all pixels with using only the pixel with the maximum artifact confidence, which directs

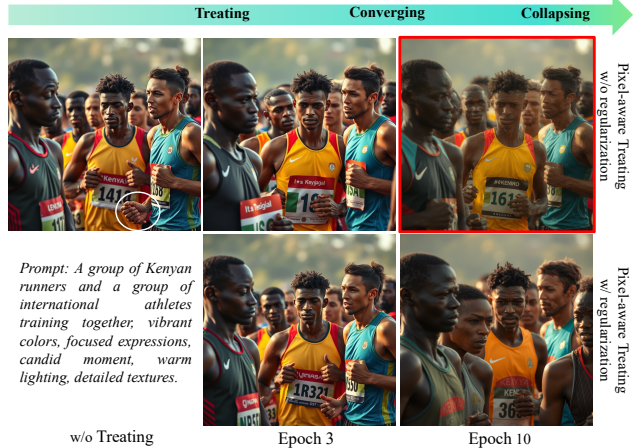


Figure 5. **DiffDoctor’s impact across epochs.** These images are synthesized by FLUX.1 during treating with or without offline regularization in evaluation time, using the same unseen prompt and seed across specific epochs of tuning. We frame the synthesized image in the model collapse stage with a red box.

the focus of treating toward the most significant error. We plot the trend of aggregated confidence changes during evaluation in Fig. 4. Using all pixels for treating converges faster and demonstrates greater stability during the first few epochs compared to selecting only the pixel with the highest confidence. Although using only the highest confidence pixel is more unstable in the initial epochs, it ultimately converges to similar confidence levels after 10 epochs. Therefore, we opt to use all pixels to achieve more stable training and faster convergence.

We further study the impacts of treating with or without offline regularization in Fig. 5. We tune FLUX.1 and observe outputs conditioned on a specific unseen prompt and the same seed in evaluation time. Before treating, the model generates an image with obvious artifacts. After 3 epochs of treating, artifacts are reduced both with or without regularization. For DiffDoctor *without* regularization, the layout of the image changes slightly when trained for epochs. But on epoch 10 it starts synthesizing overly smooth patterns that harm the image quality, which we call collapse. This corresponds to the curve of treating on all pixels in Fig. 4 around epoch 10, where the artifact confidence is almost converged. Though overly optimizing still forcibly reduces confidence, it harms the generation quality. For treating *with* regularization, it’s more stable against collapse when trained for the same 10 epochs, as the quality remains unchanged. Additionally, the image layout shifts more noticeably by epoch 10, which we attribute to the additional supervised signals introduced by the regularization term. But overly optimizing to epoch 30 still degrades the image quality (we put visualizations in the appendix), so we conclude that offline regularization can delay the collapse but can’t prevent it forever. These observations indicate that model collapse can be directly

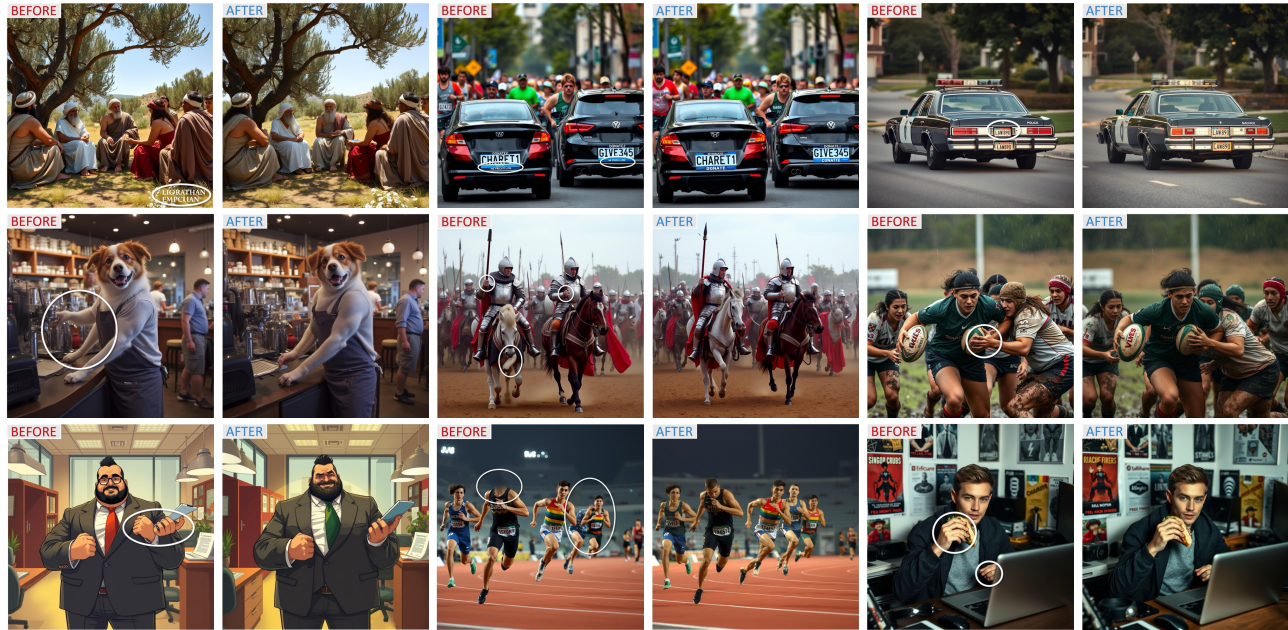


Figure 6. **DiffDoctor on FLUX.1**. All images are synthesized based on randomly generated unseen prompts not involved in training, and on the same seeds for the corresponding images before and after `DiffDoctor`. After treating, artifacts in images are reduced, but the content and layouts of the images are almost unchanged, demonstrating the effectiveness of pixel-aware treating.

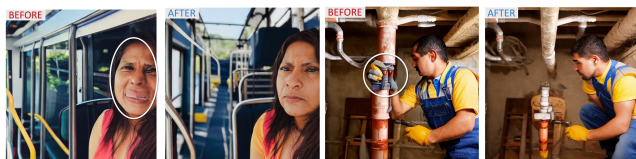


Figure 7. **DiffDoctor on SD1.5**. Images are synthesized using SD1.5 on unseen prompts not involved in `DiffDoctor` training.

Method	Mean Artifact Conf.↓	Max Artifact Conf.↓	ImageReward↑
FLUX.1 Baseline	1.56%	38.06%	1.18
+ DiffDoctor w/o Reg.	0.47%	2.36%	1.14
+ DiffDoctor w/ Reg.	0.44%	1.40%	1.16
SD1.5 Baseline	6.51%	79.37%	0.35
+ DiffDoctor w/o Reg.	5.96%	73.65%	0.33

Table 2. **DiffDoctor quantitative results**. We compare metrics before and after `DiffDoctor`, averaged on 400 images synthesized on 100 prompts featuring complex scenarios.

prevented by early stopping. Using offline regularization can *slow* the collapse, but it may shift the output distribution (image layouts) more significantly, which is not considered a drawback. Therefore, choosing to use offline regularization or not depends on the need. If we don't want to change the output distribution of the treated model too much, then we can just apply treating without offline regularization and early stopping. But if we want to optimize for more time, then we should use offline regularization.

### 4.3. Qualitative Results

**DiffDoctor on FLUX.1**. We diagnose then treat FLUX.1 in Fig. 6. All images are synthesized on unseen prompts and the same seeds for corresponding images in evaluation

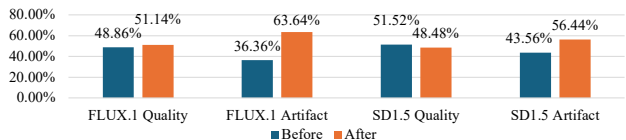


Figure 8. **User studies**. We do user studies on 24 people, making them select a winner between two images (the same diffusion model but before and after treating) based on quality or artifacts.

time. We use early stopping to prevent model collapse as discussed in Sec. 4.2. In Fig. 6, each image pair shows images synthesized before and after treating. `DiffDoctor` successfully generalizes to unseen prompts, where different kinds of artifacts (e.g., watermarks, distorted words, extra limbs, distorted hands, abnormal fingers, blurry head) that are of similar types in training time are suppressed in evaluation time, even when the scenarios are rich in details and complex patterns. We also observe that treating the model doesn't significantly change the layout of the images synthesized on the same prompt and seed in evaluation time. Pixel-aware treating seems like 'altering' the critical areas precisely to make the model avoid artifacts for these areas and other regions that are considered as low artifact confidence areas are not greatly modified.

**DiffDoctor on SD1.5**. We then perform pixel-aware treating on SD1.5 in Fig. 7. Though not as impressive as FLUX.1, treating SD1.5 provides us with valuable insights. We observe that `DiffDoctor` can reduce artifacts but cannot significantly eliminate them, and the image layouts show greater variation compared with FLUX.1. An interesting phenomenon happens in the second example, where the



Figure 9. **DiffDoctor on DreamBooth.** We perform DiffDoctor on the instance prompt and evaluate other various prompts.

model appears to take a ‘shortcut’ by omitting the man’s right hand to avoid artifacts. We assume this is due to the inferior potential of SD1.5, and the *punishment essence* of DiffDoctor:

DiffDoctor treats the model by ‘punishing what it has done’ instead of ‘forcing it to do’, so it doesn’t teach the diffusion model new concepts. This is also similar to the difference between RLHF and supervised fine-tuning. Then the cause of shortcuts is clear: SD1.5 struggles to synthesize realistic-looking hands in most cases, but when it happens to generate images with fewer hands, artifact confidence decreases, leading to less punishment. This incentivizes the diffusion model to take a shortcut by avoiding hands. In contrast, FLUX.1 has the potential to generate realistic hands, allowing it to be encouraged to improve hand synthesis without needing to avoid them.

**DiffDoctor on DreamBooth** We apply DiffDoctor to DreamBooth [21] to show that it can be used not only with plain text-to-image diffusion models in Fig. 9. Specifically, we train DreamBooth on FLUX.1 Dev using LoRA, with an inference step of 10. Then we further optimize these LoRA layers using DiffDoctor based on the instance prompt (e.g., “A [v] man”) and class prompts (e.g., “A man sits in the park”). Afterward, we evaluate various prompts describing the instance (e.g., “A [v] man eats hamburgers”). Results show that treating DreamBooth successfully reduces artifacts on unseen prompts without affecting the learned representation of the instance in DreamBooth.

#### 4.4. Quantitative Results

We use early stopping to collect the quantitative results not in the model collapse stage in Tab. 2 during evaluation.

**DiffDoctor on FLUX.1.** In Tab. 2, DiffDoctor significantly lowers the mean and the max artifact confidence after treat-

ing, while keeping the image quality as the ImageReward score changes very slightly. User studies in Fig. 8 further prove that DiffDoctor successfully reduces artifacts while keeping image quality. The winning rates on quality are almost the same, but after treating, the winning rates on artifacts significantly outperform the FLUX.1 baseline.

We also have an interesting finding that, when using offline regularization in treating, the ImageReward score rises abnormally during the model collapse stage. We provide data and visualizations in the appendix and speculate that ImageReward may also be ‘hacked’ by our method, despite not being involved in our training process.

**DiffDoctor on SD1.5.** In Tab. 2, the mean and max artifact confidence is reduced after treating for SD1.5, but not as significant as those for FLUX.1. Similarly, the winning rates on artifacts in user studies improve but are not as impressive as those for treating FLUX.1. These further verify the punishment essence of DiffDoctor, as pixel-aware treating pushes the model to avoid artifacts by punishing its outputs and thus exploiting its potential. However, it doesn’t teach the model new things. Therefore, the quantitative improvement brought by DiffDoctor is limited by the potential of SD1.5.

## 5. Conclusion and Discussion

We present `DiffDoctor`, which, to the best of our knowledge, is the first approach to use pixel-level feedback for tuning diffusion models. DiffDoctor diagnoses artifacts in synthesized images and treats the diffusion model to make them try to avoid generating artifacts in the future. To diagnose pixel-level artifacts, we train a robust artifact detector by balancing the distribution and scaling up in a human-in-the-loop manner. To treat the diffusion model, we supervise the diffusion model with the artifact detector. Experiments show that, tuned on limited prompts, DiffDoctor effectively reduces the occurrence of artifacts of similar kinds while maintaining image quality on unseen prompts, validated by qualitative and quantitative results. It is also applicable to other methods such as DreamBooth. DiffDoctor serves as a new post-training paradigm to improve the generation ability of pre-trained image diffusion models.

Despite impressive results, DiffDoctor should benefit from a more powerful artifact detector to diagnose and treat more semantically challenging abnormalities, ideally a multi-modal model capable of complex reasoning to find regions against general knowledge. Moreover, DiffDoctor can only treat the kinds of artifacts that appear in the diagnose-then-treat training process, but due to computation resources limitations, we cannot perform the training on prompts of large scales. We believe that tuning on millions of prompts across universal scenarios that cover more kinds of artifacts can further unleash the power of DiffDoctor, which we leave for future studies.



## References

- [1] Jinze Bai, Shuai Bai, Yunfei Chu, Zeyu Cui, Kai Dang, Xiaodong Deng, Yang Fan, Wenbin Ge, Yu Han, Fei Huang, et al. Qwen technical report. *arXiv:2309.16609*, 2023. 4, 5
- [2] Jinze Bai, Shuai Bai, Shusheng Yang, Shijie Wang, Sinan Tan, Peng Wang, Junyang Lin, Chang Zhou, and Jingren Zhou. Qwen-vl: A versatile vision-language model for understanding, localization, text reading, and beyond. *arXiv:2308.12966*, 2023. 4
- [3] James Betker, Gabriel Goh, Li Jing, Tim Brooks, Jianfeng Wang, Linjie Li, Long Ouyang, Juntang Zhuang, Joyce Lee, Yufei Guo, et al. Improving image generation with better captions. <https://cdn.openai.com/papers/dall-e-3.pdf>, 2023. 1
- [4] Kevin Black, Michael Janner, Yilun Du, Ilya Kostrikov, and Sergey Levine. Training diffusion models with reinforcement learning. In *ICLR*, 2024. 1, 2
- [5] Bin Cao, Jianhao Yuan, Yexin Liu, Jian Li, Shuyang Sun, Jing Liu, and Bo Zhao. Synartifact: Classifying and alleviating artifacts in synthetic images via vision-language model. *arXiv:2402.18068*, 2024. 1, 2
- [6] Kevin Clark, Paul Vicol, Kevin Swersky, and David J. Fleet. Directly fine-tuning diffusion models on differentiable rewards. In *ICLR*, 2024. 1, 2, 4
- [7] Patrick Esser, Sumith Kulal, Andreas Blattmann, Rahim Entezari, Jonas Müller, Harry Saini, Yam Levi, Dominik Lorenz, Axel Sauer, Frederic Boesel, et al. Scaling rectified flow transformers for high-resolution image synthesis, march 2024. URL <http://arxiv.org/abs/2403.03206>, 2024. 4
- [8] Ying Fan, Olivia Watkins, Yuqing Du, Hao Liu, Moonkyung Ryu, Craig Boutilier, Pieter Abbeel, Mohammad Ghavamzadeh, Kangwook Lee, and Kimin Lee. Reinforcement learning for fine-tuning text-to-image diffusion models. In *NeurIPS*, 2024. 1, 2
- [9] Jonathan Ho, Ajay Jain, and Pieter Abbeel. Denoising diffusion probabilistic models. In *NeurIPS*, 2020. 1
- [10] Edward J Hu, yelong shen, Phillip Wallis, Zeyuan Allen-Zhu, Yuanzhi Li, Shean Wang, Lu Wang, and Weizhu Chen. LoRA: Low-rank adaptation of large language models. In *ICLR*, 2022. 5
- [11] Wooyoung Kang, Jonghwan Mun, Sungjun Lee, and Byungseok Roh. Noise-aware learning from web-crawled image-text data for image captioning. In *ICCV*, 2023. 1
- [12] Yuval Kirstain, Adam Polyak, Uriel Singer, Shahbuland Matiana, Joe Penna, and Omer Levy. Pick-a-pic: An open dataset of user preferences for text-to-image generation. In *NeurIPS*, 2023. 1
- [13] Black Forest Labs. Flux.1. <https://blackforestlabs.ai>, 2024. 1, 5
- [14] Youwei Liang, Junfeng He, Gang Li, Peizhao Li, Arseniy Klimovskiy, Nicholas Carolan, Jiao Sun, Jordi Pont-Tuset, Sarah Young, Feng Yang, et al. Rich human feedback for text-to-image generation. In *CVPR*, 2024. 1, 2, 3, 4
- [15] Tsung-Yi Lin, Michael Maire, Serge Belongie, James Hays, Pietro Perona, Deva Ramanan, Piotr Dollár, and C Lawrence Zitnick. Microsoft coco: Common objects in context. In *ECCV*, 2014. 5
- [16] Xingchao Liu, Chengyue Gong, and Qiang Liu. Flow straight and fast: Learning to generate and transfer data with rectified flow. In *ICLR*, 2023. 1, 4
- [17] Long Ouyang, Jeffrey Wu, Xu Jiang, Diogo Almeida, Carroll Wainwright, Pamela Mishkin, Chong Zhang, Sandhini Agarwal, Katarina Slama, Alex Ray, et al. Training language models to follow instructions with human feedback. In *NeurIPS*, 2022. 2
- [18] Mihir Prabhudesai, Anirudh Goyal, Deepak Pathak, and Katerina Fragkiadaki. Aligning text-to-image diffusion models with reward backpropagation. *arXiv:2310.03739*, 2023. 1, 2, 4
- [19] Rafael Rafailov, Archit Sharma, Eric Mitchell, Christopher D Manning, Stefano Ermon, and Chelsea Finn. Direct preference optimization: Your language model is secretly a reward model. In *NeurIPS*, 2024. 2
- [20] Robin Rombach, Andreas Blattmann, Dominik Lorenz, Patrick Esser, and Björn Ommer. High-resolution image synthesis with latent diffusion models. In *CVPR*, 2022. 1, 5
- [21] Nataniel Ruiz, Yuanzhen Li, Varun Jampani, Yael Pritch, Michael Rubinstein, and Kfir Aberman. Dreambooth: Fine tuning text-to-image diffusion models for subject-driven generation. In *CVPR*, 2023. 2, 8
- [22] Christoph Schuhmann, Romain Beaumont, Richard Vencu, Cade Gordon, Ross Wightman, Mehdi Cherti, Theo Coombes, Aarush Katta, Clayton Mullis, Mitchell Wortsman, et al. Laion-5b: An open large-scale dataset for training next generation image-text models. In *NeurIPS*, 2022. 5
- [23] John Schulman, Filip Wolski, Prafulla Dhariwal, Alec Radford, and Oleg Klimov. Proximal policy optimization algorithms. *arXiv:1707.06347*, 2017. 2
- [24] Bram Wallace, Meihua Dang, Rafael Rafailov, Linqi Zhou, Aaron Lou, Senthil Purushwalkam, Stefano Ermon, Caiming Xiong, Shafiq Joty, and Nikhil Naik. Diffusion model alignment using direct preference optimization. In *CVPR*, 2024. 1, 2
- [25] Sheng-Yu Wang, Oliver Wang, Andrew Owens, Richard Zhang, and Alexei A Efros. Detecting photoshopped faces by scripting photoshop. In *CVPR*, 2019. 2
- [26] Xiaoshi Wu, Yiming Hao, Keqiang Sun, Yixiong Chen, Feng Zhu, Rui Zhao, and Hongsheng Li. Human preference score v2: A solid benchmark for evaluating human preferences of text-to-image synthesis. *arXiv:2306.09341*, 2023. 1
- [27] Enze Xie, Wenhai Wang, Zhiding Yu, Anima Anandkumar, Jose M Alvarez, and Ping Luo. Segformer: Simple and efficient design for semantic segmentation with transformers. In *NeurIPS*, 2021. 4
- [28] Jiazheng Xu, Xiao Liu, Yuchen Wu, Yuxuan Tong, Qinkai Li, Ming Ding, Jie Tang, and Yuxiao Dong. Imagereward: Learning and evaluating human preferences for text-to-image generation. In *NeurIPS*, 2024. 1, 2, 5
- [29] Zhipei Xu, Xuanyu Zhang, Runyi Li, Zecheng Tang, Qing Huang, and Jian Zhang. Fakeshield: Explainable image forgery detection and localization via multi-modal large language models. *arXiv:2410.02761*, 2024. 2
- [30] Lihe Yang, Wei Zhuo, Lei Qi, Yinghuan Shi, and Yang Gao. St++: Make self-training work better for semi-supervised semantic segmentation. In *CVPR*, 2022. 4

- [31] Lihe Yang, Lei Qi, Litong Feng, Wayne Zhang, and Yinghuan Shi. Revisiting weak-to-strong consistency in semi-supervised semantic segmentation. In *CVPR*, 2023. 4
- [32] Lihe Yang, Bingyi Kang, Zilong Huang, Xiaogang Xu, Jiashi Feng, and Hengshuang Zhao. Depth anything: Unleashing the power of large-scale unlabeled data. In *CVPR*, 2024. 2, 4
- [33] Lihe Yang, Bingyi Kang, Zilong Huang, Zhen Zhao, Xiaogang Xu, Jiashi Feng, and Hengshuang Zhao. Depth anything v2. In *NeurIPS*, 2024. 4
- [34] Zeqin Yu, Jiangqun Ni, Yuzhen Lin, Haoyi Deng, and Bin Li. Diffforensics: Leveraging diffusion prior to image forgery detection and localization. In *CVPR*, 2024. 2
- [35] Lingzhi Zhang, Yuqian Zhou, Connelly Barnes, Sohrab Amirghodsi, Zhe Lin, Eli Shechtman, and Jianbo Shi. Perceptual artifacts localization for inpainting. In *ECCV*, 2022. 2
- [36] Lingzhi Zhang, Zhengjie Xu, Connelly Barnes, Yuqian Zhou, Qing Liu, He Zhang, Sohrab Amirghodsi, Zhe Lin, Eli Shechtman, and Jianbo Shi. Perceptual artifacts localization for image synthesis tasks. In *ICCV*, 2023. 1, 2, 3, 4
- [37] Yanan Zhang, Eric Tzeng, Yilun Du, and Dmitry Kislyuk. Large-scale reinforcement learning for diffusion models. In *NeurIPS*, 2024. 1, 2